annalen der physik
www.ann-phys.org

Advances in Searching for Galactic Axions with a Dielectric Haloscope (MADMAX)

Antonios Gardikiotis and MADMAX Collaboration*

Axions are hypothetical particles that could explain the observed dark matter density and, simultaneously, could naturally resolve the strong charge parity (CP) problem in quantum chromodynamics (QCD). Recent theoretical works indicate that axions are expected to have masses in the range of $40-400\ \mu$eV, a range that presently still evades experimental detection. An experimental design is presented to search for QCD axions in this mass range via the magnetized disk and mirror axion experiment (MADMAX). MADMAX will be composed of multiple movable dielectric disks and a stable mirror that are placed inside a strong magnetic field to utilize the axion-induced coherent electromagnetic wave emissions from each disk surface. In this paper, new R&D milestones achieved will be reported, that is, the updated magnet quench protection system, a closed booster dielectric haloscope system tested in the MORPURGO magnet at (European Organization for Nuclear Research) CERN using a full experimental data acquisition chain. These new main novel accomplishments investigate the feasibility of the experiment.

1. Introduction

Many astrophysical observations support the hypothesis that ≈85% of the matter of the Universe is composed of dark matter (DM). The nature of this new form of matter is not part of the standard model and couples feebly with baryonic matter and radiation. One of the most appealing DM candidate particles is the axion, initially proposed as an elegant solution to the strong CP problem. The (QCD) Lagrangian includes an effective $\bar{\theta}$ parameter that introduces CP-violating observables such as the nuclear electric dipole moment (EDM) of protons and neutrons.

$$\mathcal{L}_\theta = -\frac{a_s}{8\pi}\bar{\theta}G_{\mu\nu\alpha}\tilde{G}_\alpha^{\mu\nu}, -\pi \le \bar{\theta} \le \pi \tag{1}$$

with a_s the strong coupling constant and $G_{\mu\nu\alpha}$ and $\tilde{G}_\alpha^{\mu\nu}$ is the gluon field strength tensor and its dual.

A. Gardikiotis,
Faculty of Mathematics, Informatics and Natural Sciences
Institut für Experimentalphysik
Universität Hamburg
22762 Hamburg, Germany
E-mail: antonios.gardikiotis@cern.ch

DOI: 10.1002/andp.202300046

Measurements on the neutron electric dipole moment (nEDM) have set stringent limits on the value of $\bar{\theta} \le 10^{-10}$.[1] The observed extremely small value of $\bar{\theta}$ compared to the expected value of O(1) is the so-called strong CP problem. To solve the strong CP-problem, Peccei and Quinn (PQ)[2,3] introduced a global chiral symmetry $U(1)_{PQ}$, that is spontaneously broken at scale f_a and leads to the existence of a new light spin 0 particle, the axion.[4,5] The axion mass is related to the PQ scale f_a as

$$m_a = 5.7\left(\frac{10^9}{f_a}\right)\text{meV} \tag{2}$$

Unfortunately, the theory does not predict the axion mass m_α, but axion production in early Universe and its evolution reveals that their properties are consistent with the cosmological observed cold dark matter (CDM) density.[6,7] The allowed m_a range that can produce the current cold dark matter (CDM) density, depends on whether the PQ symmetry breaking occurred before or after inflation. A plausible way to detect Galactic halo axions related to the pre-inflationary scenario, is by using tunable high-Q resonant cavities (haloscopes) permeated by a strong, static B field. The most sensitive haloscopes today are microwave cavity experiments as ADMX,[8] HAYSTAC,[9] CAST-CAPP[10] at the $1-26\ \mu$eV axion mass range. Typically, the lowest transverse magnetic mode of the cavity should match the Compton wavelength of the axion, so the coupling of the axion-induced electric field inside the cavity should be maximized. However, for axion masses above 10 GHz ($m_\alpha \ge 40\ \mu$eV) cavity haloscopes suffer from sensitivity loss due to the reduction in volume and low Q-factor. For resonant conditions the diameter of the cavity should match the half wavelength of the axion induced E-field.

In case that the PQ symmetry is broken after inflation (post-inflationary scenarios), the realignment mechanism along with decaying topological defects, provides the current axion CDM density if the axion mass is of the order of ≈100 μeV.[11,12] A recent study of lattice QCD using the post-inflationary PQ symmetry breaking scenario, favor an axion mass in the range $m_\alpha = 26\ \mu$eV to 2.3 meV,[13] if axions constitute the observed CDM density. This target axion mass range can be experimentally accessed by the dielectric haloscope, a concept that is followed by the magnetized disk and mirror axion experiment (MADMAX).[14] In this article, the concept of dielectric haloscopes, and in particular MADMAX, along with recent R&D

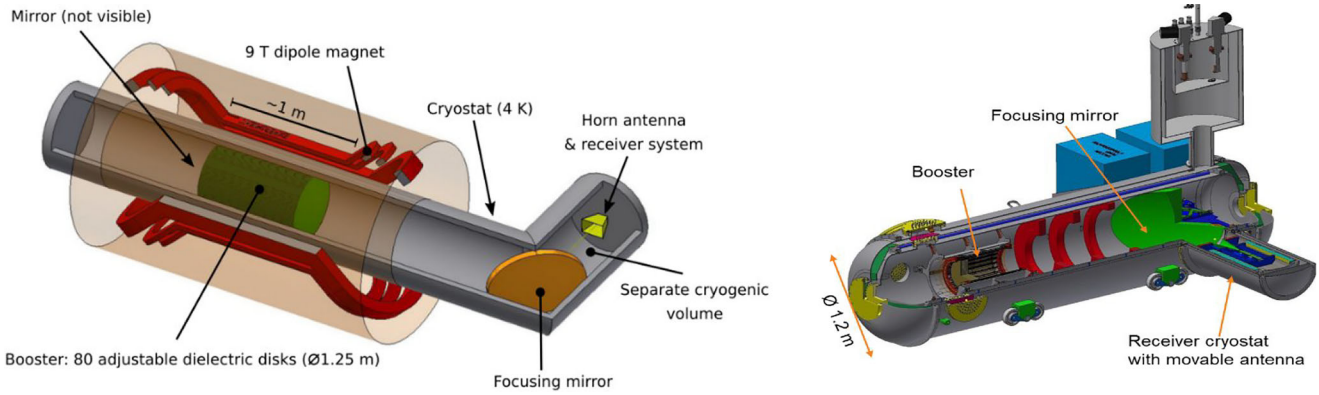

Figure 1. Left: Sketch of the final MADMAX baseline design. Right: The prototype cryostat of MADMAX. The prototype cryostat will be attached to a separate receiver cryostat that will contain a movable antenna. The receiver cryostat is under construction. The prototype cryostat can accommodate different prototype booster systems.

upgrades and first test measurements, will be discussed. In the pre-inflationary symmetry breaking scenario, smaller masses are also possible.

1.1. Dielectric Haloscope

The dielectric haloscope approach can circumvent the limitations produced in microwave cavities at high frequencies. We assume that QCD axions are bound to our galaxy and provide the local DM density of ≈0.45 cm^{-3}. The velocity dispersion of axions on Earth is given by the galactic virial velocity $\approx 10^{-3}$ c. Therefore, the corresponding de Broglie wavelength is $\lambda_{dB} = 2\pi/(m_a v_a) \approx$ 12 m. In that sense, the expected axion behaves as a homogeneous and monochromatic classical oscillating field with frequency $\nu_a = m_a/2\pi$ in the microwave range. If there is a medium with constant dielectric permittivity ϵ and permeability $\mu = 1$ inside a homogeneous static B-field B_e, the axion field induces a tiny oscillating electric field.

$$E_a(t) = \frac{g_{a\gamma}}{\epsilon} B_e a(t) \tag{3}$$

where $a(t)$ is the axion field, B_e is the external magnetic field, and $g_{a\gamma}$ is the axion-photon coupling. The electric field E_a is maximum in vacuum (for example, $E_{a0} = 1.3 \times 10^{-13}$ V m^{-1} for a 10 T magnetic field) and zero inside a metal. Axion-modified Maxwell equations do not allow the axion induced $E_a(t)$ field to be discontinuous at the boundary between media with different dielectric permittivity. To satisfy usual continuity requirements at the boundary of media with different ϵ, traveling EM waves of frequency ν_a must be emitted perpendicular to the boundary.[15] The power emitted from a single metallic mirror having area A inside a magnetic field B_e parallel to the mirror surface can be calculated by the relation:

$$P_0 = 2.2 \times 10^{-27}\mathrm{W}\left(\frac{A}{1\mathrm{m}^2}\right)\left(\frac{B_e}{10\mathrm{T}}\right)^2\left(\frac{\rho_a}{0.3\mathrm{cm}^{-3}}\right)C_{a\gamma}^2 \tag{4}$$

where ρ_a is the local axion DM density and $C_{a\gamma}$ is a model-dependent coupling constant proportional to the axion–photon coupling $g_{a\gamma}$ of the order of $O(1)$. The dielectric haloscope exploits the constructive interference effect of EM radiation emitted by many dielectric disks in front of the metallic mirror as well as a resonant enhancement by the proper adjustment of the dielectric disks.

$$P = P_0 \times \beta^2 = 1.1 \times 10^{-22}\mathrm{W}\left(\frac{A}{1\mathrm{m}^2}\right)\left(\frac{B_e}{10\mathrm{T}}\right)^2\left(\frac{\rho_a}{0.3\mathrm{cm}^{-3}}\right)C_{a\gamma}^2 \tag{5}$$

where $\beta^2(\nu_a)$ is the power boost factor that defines the enhancement of the extracted power from the dielectric haloscope with respect to the output power by a single magnetized mirror.[16] MADMAX haloscope will be composed of a booster system that accommodates 80 $LaAlO_3$ ($\epsilon \approx 24$) movable disks with a diameter of ≈1 m^2, and a 4K cryostat that houses the booster, a focusing mirror, and a horn antenna. The cryostat will be positioned inside a ≈9 T superconducting dipole magnet with a warm bore opening of 1.35 m in diameter (**Figure 1** (Left)).

1.2. MADMAX Magnet Updates

A prerequisite for reliable magnet operation is a proper quench protection strategy and the feasibility of the conductor production. For the conductor in copper conduit (CICC) construction capability, yield strength measurements have been performed for different levels of cold work.[17] These tests verify the feasibility of production of the MADMAX conductor using existing industrial tooling. A reliable magnet quench protection requires a well-established quench protection strategy that can potentially detect any unforeseen event that can harm the superconductive coil, much faster than the quench propagation velocity. In addition to simulated results that verify the MADMAX requirements, a dedicated setup was designed by (French Alternative Energies and Atomic Energy Commission) CEA and built by NOELL, the MADMAX Coil for Quench understanding—MACQU. The MACQU coil is equipped with voltage taps for measuring the voltage drop between different parts of the coil and a superconducting cable wounded around the coil, allowing, thanks to its superconducting transition voltage, to measure the normal zone length and thus determine the quench velocity.

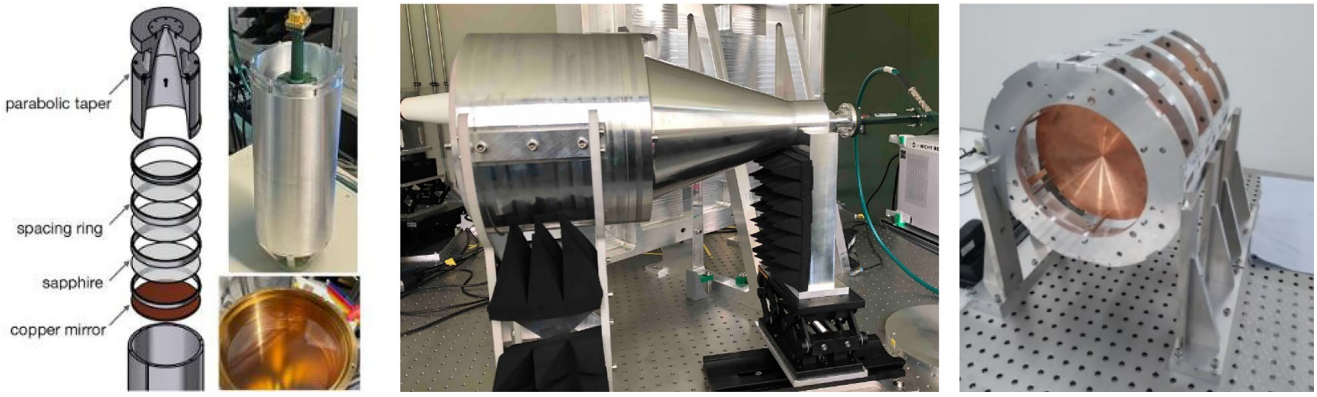

Figure 2. Left: CB100 closed booster dielectric haloscope with 3 fixed disks, optimized at 19 GHz. Center: CB200, a closed booster of 200 mm in diameter that can host up to 10 disks at fixed position. Right: P200, a minimal open booster dielectric haloscope with one movable dielectric disk and a mirror.

After extensive training tests into the CEA test cryostat, the key finding of the MACQU setup is that any quench can be safely detected faster than the quench propagation velocity $\approx 1\ s^{-1}$. This is one of the most important milestones reached for the main project risk mitigation.

Before the MADMAX magnet establishment (commissioning), the collaboration can perform competitive axion like particles (ALPs) measurements using the MORPURGO magnet at CERN in the H8 beam line at the north area. MORPURGO is a dipole magnet that can reach a maximum field of 1.6 T with a warm bore usable aperture ≈1.6 m (Figure 3 (Left)) that is available during CERN super proton synchrotron (SPS) shutdowns. The homogeneity of the field is better than 5% in the center of the magnet which fits our requirements for the prototype tests. MORPURGO has also been used for testing the mechanical feasibility of different booster setups inside its relatively strong magnetic field.

1.3. The MADMAX Prototype Cryostat

The optical system of MADMAX and the prototype booster, equipped with up to 20 solid sapphire or tiled $LaAlO_3$ disks with 300 mm diameter, should have an operational temperature ≈4 K to minimize the thermal noise of the system. Therefore, a vacuum insulated cryogenic vessel has been designed to fulfill the requirements of the MADMAX prototype cryostat (Figure 1 (Right)), that can fit in the SHielded Experimental haL (SHELL) lab in Hamburg and into the MORPURGO magnet at CERN.

The receiver system that consists of a movable horn antenna coupled to a low noise amplifier, will be housed in a separate cryostat directly connected to the main cryogenic vessel. The cryostat is cooled by 5 cryo-coolers implemented in a thermosyphon scheme. In the cold inner volume, an exchange gas like helium will be used to efficiently cool the piezo motors and the dielectric disks of the booster. The MADMAX prototype cryostat will be delivered in 2023 for commissioning at SHELL at the University of Hamburg. After successful commissioning and cryo-tests, the cryostat will be transferred to CERN for axion experiments with the MORPURGO magnet during the SPS shutdown periods in 2024–25 and potentially in 2025–26 too.

1.4. Prototyping Strategy: MADMAX Test Setups

To verify the feasibility of the final MADMAX setup the RF behavior of all individual mechanical components should be tested. The required precision set by mechanics can influence the RF response to small changes or inaccuracies and potentially affect the boost factor. Henceforth, several test setups have been designed and built, to verify the required feasibility.[20]

The closed booster 100 (CB100) in **Figure 2** (Left), is a closed metallic booster system that contains three fixed sapphire disks of 100 mm in diameter, in front of a copper mirror. CB100 has been built to provide a detailed RF understanding of a dielectric haloscope with well-defined boundary conditions. It has also been used to verify the method that provides a reliable boost factor determination.

A second closed booster CB200 that can accommodate up to 10 fixed dielectric disks of 200 mm in diameter is shown in Figure 2 (Center). CB200 has been built and it is currently under study. Furthermore, CB200 has been designed to be used in an open booster configuration, thus providing additional information that can assess the differences between open and closed system conditions. Finally, measurements on both configurations provide crucial input to the simulations performed.[18] to verify the boost factor. An open booster setup, Project 200 (P200), will also be used for RF measurements to study the Electromagnetic (EM) response, following dedicated simulations. P200 is composed of a single sapphire disk and a copper mirror inside a backbone structure (Figure 2 (Right)). In addition, it can also accommodate a tiled disk, made of glued hexagon tiles instead of using a single crystal disk.[19]

1.5. Mechanics Prototype: R&D Updates on P200

P200 has been used as technological proof of principle and R&D setup to demonstrate the mechanical feasibility of the MADMAX final design. On this setup, the required precision of the individual disks that can be moved in front of the copper mirror by the piezo motors, at cryogenic temperatures and in B-field has been achieved. P200 contains an integrated cryogen-proof interferometer capable of measuring the disk position at three points with

a precision better than 1 μm. The sapphire disk is mounted to a titanium ring, and it is connected to three motor carriages that can slide on rails attached to the P200 backbone structure. The feasibility of operating the piezo motors at cryogenic temperatures ≈ 4.5 K and in a strong B-field of 5.3 T has been evaluated using an ALPS test magnet at deutsches elektronen-synchrotron (DESY). After successful room temperature tests, P200 is transported at CERN to verify the functioning of the P200 assembly at cryogenic temperatures and in 1.6 T magnetic field in the MORPURGO magnet. P200 successfully tested at CERN's cryolab and in MORPURGO magnet, providing that the laser interferometer worked at cryogenic temperatures and that the backbone structure keeps the optics alignment during cool down. The dielectric disk of a minimal dielectric haloscope can be routinely moved with the required precision using the interferometer feedback in extreme conditions. Therefore, the mechanical feasibility and the R&D milestones of P200 have been achieved.

1.6. RF Studies and Measurements

P200 can be used to study the RF behavior of a minimal open booster system with one dielectric disk. The closed booster measurements of CB100 and CB200 along with verified simulations will advance the RF modeling of an open booster system like P200 and the future more complex prototypes.

One of the most important aspects of the dielectric haloscopes is the understanding of their RF behavior and the boost factor estimation. Since the boost factor cannot be directly measured, indirect methods to assess the boost factor utilizing accessible parameters from simulations and measurements can be used. Mechanical inaccuracies or any possible impedance mismatch of the system could potentially limit the boost factor. To probe the boost factor and estimate the uncertainties of the system, reflectivity and thermal noise measurements can provide the key parameters correlated with the boost factor. The reflectivity of the system is calculated by an analytical 1D model.[20] 3D simulations can also evaluate the reflectivity of the system. A good agreement between 1D model, 3D simulations, and the measured reflectivity can validate the model and the boost factor derived.

In addition to the reflectivity measurements, the total system noise T_{sys} can give valuable information of the system response. T_{sys} depends on the booster configuration and the receiver system, that is, $T_{sys} = T_{booster} + T_{receiver}$, and it is also correlated to the boost factor. Noise that is emitted by the pre-amplifier into the booster system and then it is back reflected, leads to constructive or destructive interference that depends on the system geometry (booster) and the material properties. The overall thermal radiation is correlated to the boost factor since it is mainly emitted by the copper mirror and the disks surfaces. Such measurements, in addition to calibration measurements of the pre-amplifier, can provide the most relevant parameters for the boost factor calculation.

To perform data measurements a full heterodyne DAQ (data acquisition) system has been built and optimized to the booster peak bandwidth at ≈19 GHz. This HEMT (high electron mobility transistor)-based receiver consists of four time-shifted digital 16-bit samplers and internal field programmable gate arrays (FPGAs) for fast fourier transform (FFT) real time calculation providing a dead time of <2%.

CB100 test measurements have been performed in 2022 inside the 1.6 T B-field of the MORPURGO magnet at CERN (**Figure 3** (Left)) to test the receiver chain and the DAQ system at room temperature. The data taking tests performed to estimate the radio frequency interference (RFI) effects and to establish a proper data storage and a functional data analysis methodology. After the completion of the data analysis pipeline, CB100 can be used for long run data taking that can lead to a new projection limit in ALP space.

The measurement tests performed during the MORPURGO magnet upgrades and commissioning period, therefore the data taking time was quite short for any real physics measurement. The tests performed, used for (Radio Frequency Intereference) RFI identification inside and outside the MORPURGO warm bore (with magnet on and off) and for the comparison of the spectra taken at CERN and in the MPP laboratory. The MADMAX data of the CB100 setup at CERN verified that there is no impeded RF behavior (Figure 3 (Right)). It could be shown that the highly sensitive receiver could be operated close to the magnet area and RFI measurements cannot influence the performance of the heterodyne mixing scheme. System noise measurements in the MORPURGO magnet with magnetic field on and off does not alter the calibration measurements obtained in the lab. Therefore, there is no influence of the B-field on the CB100 system and its RF response.

1.7. Project Plans and Conclusions

MADMAX will use the MORPURGO magnet at CERN to run competitive physics measurements using the CB100 and possibly the CB200 setups. In 2023, it is expected that the MORPURGO magnet upgrades will provide a stable 1.6 T dipole field over the course of days or weeks. The beam shut down period in 2024 can be used to perform long term measurements even at cryogenic temperatures. Long term data could provide competitive ALPs limits for $m_a \approx 78.6$ μeV and a sensitivity to ALP photon coupling $g_{a\gamma} < 3.4 \times 10^{-11}\text{GeV}^{-1}$ provided that the power boost factor is $\beta^2 = 800$ at a system temperature $T_{sys} = 200$ K and for integration time $\tau = 10$ days. The achieved sensitivity will exceed the (Cern Axion Solar Telescope) CAST limit[21] in the given mass region by a factor of two. Similar long-term measurements without magnetic field for hidden photon search can also provide limits of the kinematic mixing parameter χ in an unexplored parameter space at the same frequency range.

In conclusion, the major R&D milestones of MADMAX have been reached.

Limits already achieved are displayed by solid lines (CAST helioscope and cavity experiments), projected sensitivities are displayed in dashed lines. Projections in the orange QCD region define the pre-inflationary scenario accessible by cavity experiments (CAPP, ADMX). The dielectric haloscope can scan a wide range preferred by the post-inflationary scenario.

A method to assess the power boost factor and its uncertainty has been shown to work on a closed booster system. In addition, the conductor for the final magnet design is suitable for safe

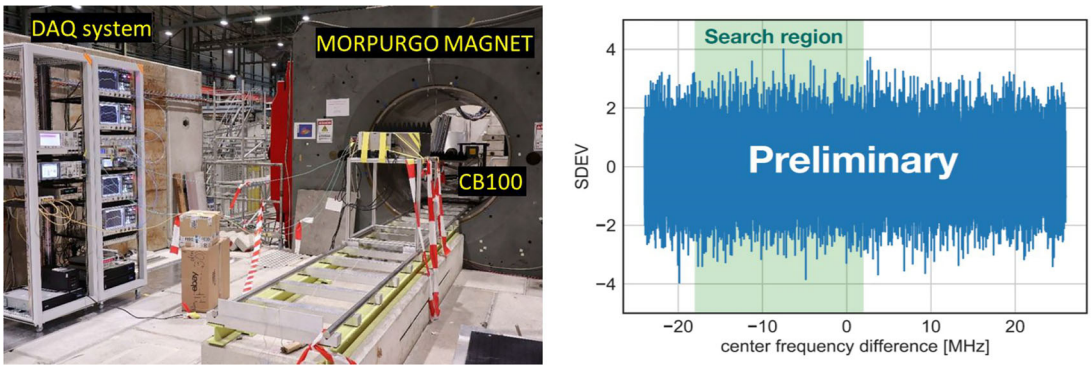

Figure 3. Left: CB100 setup including receiver and DAQ at CERN in front of the MORPURGO magnet. Right: Background measurements of the CB100 inside the MORPURGO magnet at CERN. The measured power is normalized to the noise level in terms of standard deviation (SDEV), to get the relative power of the signal above background. The search region is located around 19.25 GHz.

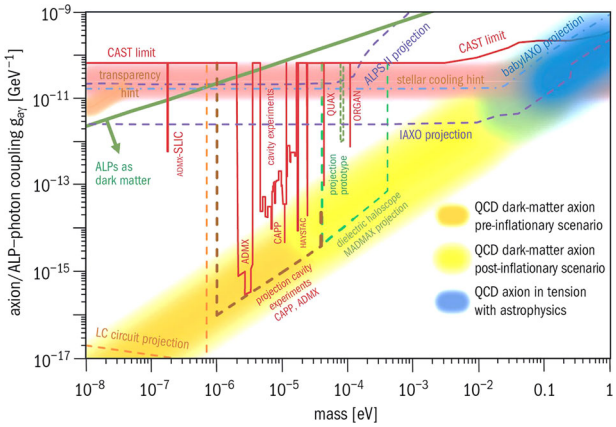

Figure 4. Experimental exclusion limits on the axion–photon coupling versus axion mass.

operation in terms of a fast enough quench protection system. The enabling technologies show the feasibility of the piezo actuators to work in strong B-field and at cryogenic temperatures. The mechanical concept of the MADMAX baseline design has been verified after extensive tests on the minimal open booster setup, P200. The prototype cryostat will be delivered and installed in 2023 in the SHELL laboratory at the University of Hamburg.

MADMAX projection in sensitivity is shown in **Figure 4** along with current limits from cavity experiments and from the CAST helioscope. The QCD axions are predicted to lie on a diagonal band defined by the (Kim–Shifman–Vainshtein–Zakharov) KSVZ and (Dine–Fischler–Srednicki–Zhitnisky)DFSZ benchmark models. MADMAX aims to cover a wide range of the parameter space in the post-inflationary scenario, that is, when the Peccei–Quinn symmetry is broken after the cosmic inflation.

Acknowledgements

Open access funding enabled and organized by Projekt DEAL.

Conflict of Interest

The authors declare no conflict of interest.

Data Availability Statement

The data that support the findings of this study are available from the corresponding author upon reasonable request.

Keywords

axions, dielectric haloscope, MADMAX, microwaves

Received: January 31, 2023
Revised: March 31, 2023
Published online: May 26, 2023

[1] C. Abel, S. Afach, N. J. Ayres, C. A. Baker, G. Ban, G. Bison, K. Bodek, V. Bondar, M. Burghoff, E. Chanel, Z. Chowdhuri, P. J. Chiu, B. Clement, C. B. Crawford, M. Daum, S. Emmenegger, L. Ferraris-Bouchez, M. Fertl, P. Flaux, B. Franke, A. Fratangelo, P. Geltenbort, K. Green, W. C. Griffith, M. V. D. Grinten, Z. D. Grujić, P. G. Harris, L. Hayen, W. Heil, R. Henneck, et al., *Phys. Rev. Lett.* **2020**, *124*, 081803.
[2] R. D. Peccei, H. R. Quinn, *Phys. Rev. Lett.* **1977**, *38*, 1440.
[3] R. D. Peccei, H. R. Quinn, *Phys. Rev.* **1977**, *16*, 1791.
[4] F. Wilczek, *Phys. Rev. Lett.* **1978**, *40*, 279.
[5] S. Weinberg, *Phys. Rev. Lett.* **1978**, *40*, 223.
[6] J. Preskill, M. B. Wise, F. Wilczek, *Phys. Lett. B* **1983**, *120*, 127.
[7] J. Jaeckel, A. Ringwald, *Ann. Rev. Nucl. Part. Sci.* **2010**, *60*, 405.
[8] ADMX Collaboration, C. Bartram, T. Braine, E. Burns, R. Cervantes, N. Crisosto, N. Du, H. Korandla, G. Leum, P. Mohapatra, T. Nitta, L. J. Rosenberg, G. Rybka, J. Yang, J. Clarke, I. Siddiqi, A. Agrawal, A. V. Dixit, M. H. Awida, A. S. Chou, M. Hollister, S. Knirck, A. Sonnenschein, W. Wester, J. R. Gleason, A. T. Hipp, S. Jois, P. Sikivie, N. S. Sullivan, D. B. Tanner, et al., *Phys. Rev. Lett.* **2021**, *127*, 261803.
[9] B. M. Brubaker, L. Zhong, Y. V. Gurevich, S. B. Cahn, S. K. Lamoreaux, M. Simanovskaia, J. R. Root, S. M. Lewis, S. A. Kenany, K. M. Backes, I. Urdinaran, N. M. Rapidis, T. M. Shokair, K. A. V. Bibber, D. A. Palken, M. Malnou, W. F. Kindel, M. A. Anil, K. W. Lehnert, G. Carosi, *Phys. Rev. Lett.* **2017**, *118*, 061302.
[10] C. M. Adair, K. Altenmüller, V. Anastassopoulos, S. A. Cuendis, J. Baier, K. Barth, A. Belov, D. Bozicevic, H. Bräuninger, G. Cantatore, F. Caspers, J. Castel, S. Çetin, W. Chung, H. Choi, J. Choi, T. Dafni, M. Davenport, A. Dermenev, K. Desch, B. Döbrich, H. Fischer, W. Funk, J. Galan, A. Gardikiotis, S. Gninenko, J. Golm, M. Hasinoff, D. H. H. Hoffmann, D. Díez Ibáñez, *Nat. Commun.* **2022**, *13*, 6180.
[11] M. K. Hiramatsu, K. Saikawa, T. Sekiguchi, *Phys. Rev. D* **2012**, *85*, 105020.

[12] S. Borsanyi, Z. Fodor, J. Guenther, K. H. Kampert, S. D. Katz, T. Kawanai, T. G. Kovacs, S. W. Mages, A. Pasztor, F. Pittler, J. Redondo, A. Ringwald, K. K. Szabo, *Nature* **2016**, *539*, 69.
[13] G. Ballesteros, J. Redondo, A. Ringwald, C. Tamarit, *J. Cosmol. Astropart. Phys.* **2017**, *118*, 071802.
[14] A. Caldwell, G. Dvali, B. Majorovits, A. Millar, G. Raffelt, J. Redondo, O. Reimann, F. Simon, F. Steffen, MADMAX interest group, *Phys. Rev. Lett.* **2017**, *118*, 091801.
[15] D. Horns, J. Jaeckel, A. Lindner, A. Lobanov, J. Redondo, A. Ringwald, *J. Cosmol. Astropart. Phys.* **2013**, *1304*, 016.
[16] A. J. Millar, G. G. Raffelt, J. Redondo, F. D. Steffen, *J. Cosmol. Astropart. Phys.* **2017**, *1701*, 061.
[17] C. Berriaud, W. A. Maksoud, V. Calvelli, G. Dilasser, F. P. Juster, A. Madur, F. Nunio, J. M. Rifflet, L. Scola, *IEEE Trans. Appl. Supercond.* **2020**, *30*, 1.
[18] The MADMAX collaboration, S. Knirck, J. Schütte-Engel, S. Beurthey, D. Breitmoser, A. Caldwell, C. Diaconu, J. Diehl, J. Egge, M. Esposito, *J. Cosmol. Astropart. Phys.* **2021**, *2021*, 034.
[19] S. Beurthey, N. Böhmer, P. Brun, A. Caldwell, L. Chevalier, C. Diaconu, G. Dvali, P. Freire, E. Garutti, C. Gooch, A. Hambarzumjan, S. Heyminck, F. Hubaut, J. Jochum, P. Karst, S. Khan, D. Kittlinger, S. Knirck, M. Kramer, C. Krieger, T. Lasserre, C. Lee, X. Li, A. Lindner, B. Majorovits, M. Matysek, S. Martens, E. Öz, P. Pataguppi, P. Pralavorio, et al., MADMAX Collaboration [arXiv:2003.10894v2].
[20] J. Egge, S. Knirck, B. Majorovits, C. Moore, O. Reimann, *Eur. Phys. J. C* **2020**, *80*, 392.
[21] CAST Collaboration, *Nat. Phys.* **2017**, *13*, 584.